ALMA MATER STUDIORUM
UNIVERSITÀ DI BOLOGNA

ARCHIVIO ISTITUZIONALE
DELLA RICERCA

Alma Mater Studiorum Università di Bologna
Archivio istituzionale della ricerca

Hyperfine-resolved spectra of HDS together with a global ro-vibrational analysis

This is the final peer-reviewed author's accepted manuscript (postprint) of the following publication:

Published Version:
Melosso, M., Jiang, N., Gauss, J., Puzzarini, C. (2023). Hyperfine-resolved spectra of HDS together with a global ro-vibrational analysis. THE JOURNAL OF CHEMICAL PHYSICS, 158(17), 1-11 [10.1063/5.0148810].

Availability:
This version is available at: https://hdl.handle.net/11585/955025 since: 2024-01-31

Published:
DOI: http://doi.org/10.1063/5.0148810

Terms of use:

Some rights reserved. The terms and conditions for the reuse of this version of the manuscript are specified in the publishing policy. For all terms of use and more information see the publisher's website.

This item was downloaded from IRIS Università di Bologna (https://cris.unibo.it/).
When citing, please refer to the published version.

(Article begins on next page)

18 August 2024

This is the final peer-reviewed accepted manuscript of:

M. Melosso, N. Jiang, J. Gauss, and C. Puzzarini. "Hyperfine-resolved spectra of HDS together with a global ro-vibrational analysis", J. Chem. Phys. 158, 174310 (2023)

The final published version is available online at: https://doi.org/10.1063/5.0148810

Terms of use:

Some rights reserved. The terms and conditions for the reuse of this version of the manuscript are specified in the publishing policy. For all terms of use and more information see the publisher's website.

This item was downloaded from IRIS Università di Bologna (https://cris.unibo.it/)

When citing, please refer to the published version.

Hyperfine-resolved spectra of HDS together with a global ro-vibrational analysis

Mattia Melosso,[1] Ningjing Jiang,[1] Jürgen Gauss,[2] and Cristina Puzzarini[1]
[1)] *Dipartimento di Chimica "Giacomo Ciamician", Università di Bologna, via F. Selmi 2, 40126 Bologna, Italy.*
[2)] *Department Chemie, Johannes Gutenberg-Universität Mainz, Duesbergweg 10–14, 55128 Mainz, Germany.*

(*Electronic mail: cristina.puzzarini@unibo.it)

(*Electronic mail: mattia.melosso2@unibo.it)

(Dated: 31 January 2024)

Despite their chemical simplicity, the spectroscopic investigation of light hydrides such as hydrogen sulfide is challenging due to strong hyperfine interactions and/or anomalous centrifugal-distortion effects. Several hydrides have already been detected in the interstellar medium, and the list includes H_2S and some of its isotopologues. Astronomical observation of isotopic species and, in particular, those bearing deuterium is important to gain insights into the evolutionary stage of astronomical objects and to shed light on interstellar chemistry. These observations require a very accurate knowledge of the rotational spectrum, which is so far limited for mono-deuterated hydrogen sulfide, HDS. To fill this gap, high-level quantum-chemical calculations and sub-Doppler measurements have been combined for the investigation of the hyperfine structure of the rotational spectrum in the millimeter- and submillimeter-wave region. In addition to the determination of accurate hyperfine parameters, these new measurements together with the available literature data allowed us to extend the centrifugal analysis using a Watson-type Hamiltonian and a Hamiltonian-independent approach based on the Measured Active Ro-Vibrational Energy Levels (MARVEL) procedure. The present study thus permits to model the rotational spectrum of HDS from the microwave to far-infrared region with great accuracy, thereby accounting for the effect of the electric and magnetic interactions due to the deuterium and hydrogen nuclei.

I. INTRODUCTION

High-resolution spectroscopy is a powerful tool to characterize and unravel the underlying physico-chemical properties of complex molecular systems, such as those exhibiting large-amplitude motions,[1,2] flexible molecules with a rich conformational landscape,[3–7] complexes showing non-standard intermolecular bonds,[8–10] but also systems showing network(s) of anharmonic resonances,[11,12] hyperfine structures,[13,14] and/or anomalous centrifugal-distortion effects.[15,16] While most of the complexity issues mentioned above are inherent features of medium- to large-sized systems, the last two aspects are typical for small hydrides such as, for example, water (H_2O), the amidogen radical (NH_2), and the methylene radical (CH_2). As a consequence of the "floppiness" of these light species, a complete modeling of their ro-vibrational energy levels is a challenging task and is difficult to achieve with an accuracy able to reproduce and support experimental measurements. The main reason for that is the slow converge of the Watson Hamiltonian,[17,18] which is considered the gold-standard model Hamiltonian for ro-vibrational spectroscopy. The lightness of these hydrides also leads to sparse spectra, thus limiting the number of observable spectroscopic features and, consequently, the number of experimental data to compare with theory. Furthermore, the spectra of these species are often complicated by the so-called hyperfine structure, which results in the splitting of the rotational energy levels due to electric and/or magnetic interactions.[19–21] Thus, for an accurate modeling of the rotational and vibrational energy levels, proper account and description of centrifugal-distortion effects and hyperfine interactions are mandatory in many spectroscopy-based applications,[22–26] such as atmospheric measurements and astronomical observations.

Focusing on astrochemistry, several hydrides have already been detected in the interstellar medium (ISM); the list includes H_2O, NH_2, CH_2, and H_2S, as well as several of their isotopologues.[27–39] These species can be thus used to trace the chemical differentiation and complexity across our Galaxy and beyond. In addition, the observation of their isotopically substituted species – in particular deuterated species – is a useful indicator for the evolutionary stage of astronomical objects.[40–44] In this view, deuterated hydrogen sulfide (HDS) can provide new insights into the so-called "sulfur problem", i.e., the fact that the number of interstellar S-containing species is smaller than what expected from the cosmic sulfur abundance.[45–47] Furthermore, the observation of deuterium enrichment (denoted as deuterium fractionation) for a given molecular species can shed some light on its formation mechanism in the ISM, whose chemistry is very different from the terrestrial counterpart.[48–50] In view of what has been pointed out above, it is clear that an accurate characterization of the rotational spectrum of HDS is needed, which necessitates a correct interpretation of laboratory spectroscopic data in terms of spectroscopic and hyperfine parameters.

The rotational spectrum of HDS has been measured in the microwave (MW)[51–54] and far-infrared (FIR)[55] regions, but not at millimeter- and submillimeter-wavelengths, where most of the astronomical observations are carried out. Moreover, the different sources of experimental data – which include several high-resolution ro-vibrational studies[56–64] – have never been combined into a unique analysis so far, thus leading to

several, different sets of spectroscopic parameters being available in the literature.

In this work, we aim at the investigation of the ro-vibrational energy levels manifold of HDS, overcoming the aforementioned difficulties with a multi-level approach. First, we exploit high-level quantum-chemical calculations to obtain accurate theoretical estimates for the hyperfine parameters of HDS, namely the nuclear quadrupole coupling, spin-rotation, and dipolar spin-spin constants (Section II), as well as to improve the available theoretical estimates for the rotational and centrifugal-distortion terms. All these predictions are crucial to guide and support both the experiment and the spectral analysis. Subsequently, we present new accurate measurements of high-frequency pure rotational transitions of HDS observed either in direct absorption or in a saturation regime (§ III). In Section IV, we report the spectral analysis of both the literature and newly measured data using the Watson-type Hamiltonian (§ IV B) and a Hamiltonian-independent approach based on the MARVEL (Measured Active Ro-Vibrational Energy Levels) procedure[65] (§ IV C). Finally, we discuss our findings and point out the capabilities and limits of our modelling and results.

II. COMPUTATIONAL DETAILS

The selection of the transitions to be investigated at sub-Doppler resolution as well as the analysis of their hyperfine structure have been guided by quantum-chemical calculations of the corresponding hyperfine parameters. These are: the nuclear quadrupole coupling (χ_{ij}), nuclear spin-rotation (C_{ij}) and dipolar spin-spin interaction (D_{ij}) constants. Interested readers are referred to ref. 19 for a detailed account on how these hyperfine parameters can be obtained from quantum-chemical computations. To briefly summarize, HDS contains only one quadrupolar nucleus which is the deuterium having a nuclear spin I_{D} equal to one. Deuterium quadrupole-coupling constants χ_{ij} have been determined using the following expression:

$$\chi_{ij} = eQq_{ij}, \tag{1}$$

where i and j refer to the inertial axes. eQ is the deuterium quadrupole moment (2.860(15) mbarn[66]), and q_{ij} represents the ij-th element of the electric-field gradient tensor,[19] which is obtained from quantum-chemical computations as a first-order property.

Moving to nuclear spin-rotation constants, a detailed account on the corresponding quantum-chemical calculations can be found in refs. 67,68. To summarize, the electronic contribution is evaluated as the second derivative of the electronic energy with respect to the rotational angular momentum and the nuclear spin.[67,68] Perturbation-dependent basis functions,[67] also denoted as rotational London orbitals, are employed to improve the basis-set convergence. The nuclear contribution, instead, only depends on the molecular geometry.[69] The same is the case for the dipolar spin-spin coupling tensor, for which the equilibrium structure straightforwardly provides the equilibrium components. Expressions for the dipolar spin-spin interaction constants can be found in ref. 19 and quantum-chemical computations are only needed for the evaluation of vibrational corrections.

To obtain accurate theoretical predictions of the hyperfine parameters introduced above, coupled-cluster (CC) theory[70] has been exploited. In detail, the coupled-cluster (CC) singles and doubles (CCSD) approach augmented by a perturbative treatment of triple excitations (CCSD(T))[71] with all electrons (ae) correlated, has been employed in conjunction with the aug-cc-pCV5Z basis set.[72–75] Computations have been performed using the accurate equilibrium structure reported in ref. 22, which accounts for the extrapolation to the complete basis-set (CBS) limit at the CCSD(T) level, core-correlation effects evaluated with a quintuple-zeta basis set, and high-order terms in the cluster expansion (full treatment of triples and quadruples). For quantitative predictions, the ae-CCSD(T)/aug-cc-pCV5Z equilibrium values have been augmented by vibrational corrections, computed at the ae-CCSD(T)/cc-pCVQZ level. For their evaluation, an approach based on second-order vibrational perturbation theory (VPT2)[76] has been employed, which is described in detail in ref. 77.

Among the hyperfine parameters described above, the nuclear spin-rotation tensors are the most challenging to be computed quantitatively. To further improve their prediction, the following composite scheme based on the CC theory has been employed:

$$C_{\mathrm{best}} = C^{\infty}(\mathrm{SCF}) + \Delta C^{\infty}(\mathrm{CCSD(T)}) + \Delta C(\mathrm{fT}) + \Delta C(\mathrm{fQ}) \ , \tag{2}$$

where C denotes an element of the spin-rotation tensor. In the equation above, the first two terms on the right-hand side corresponds to values extrapolated to the CBS limit. In a two-step procedure, the Hartree-Fock self-consistent-field (HF-SCF) and the CCSD(T) values are extrapolated separately. The exponential expression by Feller[78] is used for the former, and the n^{-3} extrapolation scheme by Helgaker *et al.*[79] is used for the latter. The third and fourth terms of Eq. (2) provide corrections due to a full treatment of triple excitations (fT) and due to quadruple excitations (fQ), respectively. These have been evaluated as difference between the CCSDT and CCSD(T) and between the CCSDTQ and CCSDT contributions, respectively. The CCSDT and CCSDTQ acronyms here stand for CC single, double, and triple excitations,[80,81] and CC with single, double, triple, and quadruple excitations.[82,83] All computations have been performed in conjunction with the correlation-consistent aug-cc-pCVnZ basis sets,[72–75,84,85] and with all electrons correlated. For the different steps, the following values of n have been employed: n=Q,5,6 for HF-SCF, n=5,6 for CCSD(T), n=T for fT, and n=D for fQ.

To test the effect of the geometry on the equilibrium values of the hyperfine parameters, the equilibrium structure evaluated in ref. 22 has been augmented by a contribution accounting for relativistic effects. These have been treated using second-order direct perturbation theory (DPT2)[86] at the ae-CCSD(T) level in conjunction with the uncontracted version of the cc-pCVQZ set. While the bond distance nearly remains unchanged (1.3358 Å), the angle varies from 92.332 deg. to 92.238 deg. It is noted that such a variation only marginally

affects the computed hyperfine parameters (changes of the order of 0.01-0.02 kHz). Therefore, it will not be further discussed in the following.

Finally, though rotational parameters of HDS are already available in the literature,[87] in this work we report improved values for them by computing the required harmonic and anharmonic force field at the CCSD(T)/aug-cc-pCV5Z level, with all electron correlated. The harmonic force field was obtained using analytic second derivatives,[88] whereas the cubic force field was determined in a normal-coordinate representation via numerical differentiation of the analytically evaluated harmonic force constants.[89,90] By exploiting VPT2 calculations in combination with this anharmonic force field, the vibrational corrections to the rotational constants as well as the quartic and sextic centrifugal-distortion constants have been obtained. In this respect, it has to be noted that an error in the CFOUR implementation of the H_J and h_2 sextic terms (S-reduced Watson Hamiltonian[91]) has been fixed. Equilibrium rotational constants were straightforwardly derived from the improved equilibrium structure mentioned above (i.e., that from ref. 22 augmented by the relativistic corrections).

All CCSD(T) calculations have been performed using the CFOUR program package,[92,93] while the CCSDT and CCSDTQ computations have been carried out with the MRCC program[94,95] interfaced to CFOUR.

III. EXPERIMENT

New measurements of the rotational spectrum of HDS were carried out using a frequency-modulated computer-controlled spectrometer operating between 65 GHz and 1.6 THz, for which a detailed description can be found in refs. 96–98. In the present investigation, the measurements were performed in the 244 GHz - 1.59 THz frequency range at either Doppler-limited (weak lines and for most of transitions at frequency higher than 700 GHz) or sub-Doppler resolution[23,99] (Lamb-dip technique).

Briefly, spectral coverage up to 900 GHz is obtained by combining a Gunn diode working in the W band (80–115 GHz) with passive frequency multipliers (doublers and triplers in cascade). THz frequencies are produced by coupling several Gunn diodes working in the F band (115–134 GHz) to two triplers in cascade, with the 12th harmonic still detectable with an output power of a few μW. The millimeter-/submillimeter-wave radiation, stabilized and frequency-modulated in a phase-lock-loop, is fed to a 3 m long, free-space glass absorption cell. The output signal was then detected by a hot-electron InSb bolometer, filtered and demodulated at twice the modulation frequency ($2f$ detection scheme) through a lock-in amplifier, and analog-to-digital converted. The frequency accuracy of the spectra is ensured by a 5 MHz rubidium atomic clock used as reference for all the frequency synthesizers employed in the synchronization loop.

Samples of HDS were prepared via isotopic exchange by mixing similar amounts of H_2S and D_2O. To avoid the exchange of the D atoms in the sample with the H atoms of water absorbed on the cell walls, before starting a series of measurements, D_2O was first introduced and stored in the cell for a few minutes and then, after pumping it out, the mixed sample was injected. While Doppler-limited measurements were carried out under static conditions (with the cell filled with about 1 to 3 Pa of the sample mixture), the Lamb-dip ones were performed in a continuous flow of gas, maintained by a diffusion pump, in order to keep a constant pressure of 0.05-0.1 Pa inside the cell.

IV. RESULTS AND DISCUSSION

As mentioned in the Introduction, two different spectroscopic analyses have been carried out. The first one is based on a Watson-type Hamiltonian, while the second one exploits the MARVEL approach. Both of them include the results from the measurements performed in the present work, whose analysis is first of all discussed.

A. Spectral assignment

In case of the Lamb-dip measurements, the hyperfine structure of the rotational spectrum due to the deuterium and hydrogen nuclei has been resolved. The main contribution is here due to the nuclear quadrupole coupling of D with further splittings due to the spin-rotation interaction of H (nuclear spin: $I_{\text{H}} = 1/2$), while spin-rotation interactions of D only causes shifts of the already split hyperfine components. Furthermore, small but non-negligible, modifications are due

TABLE I. Comparison of experimental and computed hyperfine parameters of HDS.

Constant	Nucleus	Unit	Experiment[a]	Theory[b]
X_{aa}	(D)	MHz	0.1522(11)	0.15292
X_{bb}	(D)	MHz	−0.0646(19)	−0.06379
X_{ab}	(D)	MHz	0.01924	0.01924
C_{aa}	(D)	kHz	0.51	0.51
C_{bb}	(D)	kHz	−2.77(37)	−2.70
C_{cc}	(D)	kHz	−1.80	−1.80
C_{aa}	(H)	kHz	−37.05(39)	−35.32
C_{bb}	(H)	kHz	2.18	2.18
C_{cc}	(H)	kHz	−11.49(64)	−11.74
D_{aa}	(H-D)	kHz	−2.19	−2.19
D_{bb}	(H-D)	kHz	−0.39	−0.39

[a] Numbers in parentheses are one standard deviation in units of the last quoted digit. Values without associated error are held fixed to their computed value. **[b]** Nuclear quadrupole coupling: ae-CCSD(T)/aug-cc-pCV5Z equilibrium values. Nuclear spin-rotation: ae-CCSD(T)/CBS+fT+fQ equilibrium values. Dipolar spin-spin coupling: equilibrium values from the improved geometry (present work). All parameters are augmented by vibrational corrections computed at the ae-CCSD(T)/aug-cc-pCVQZ level.

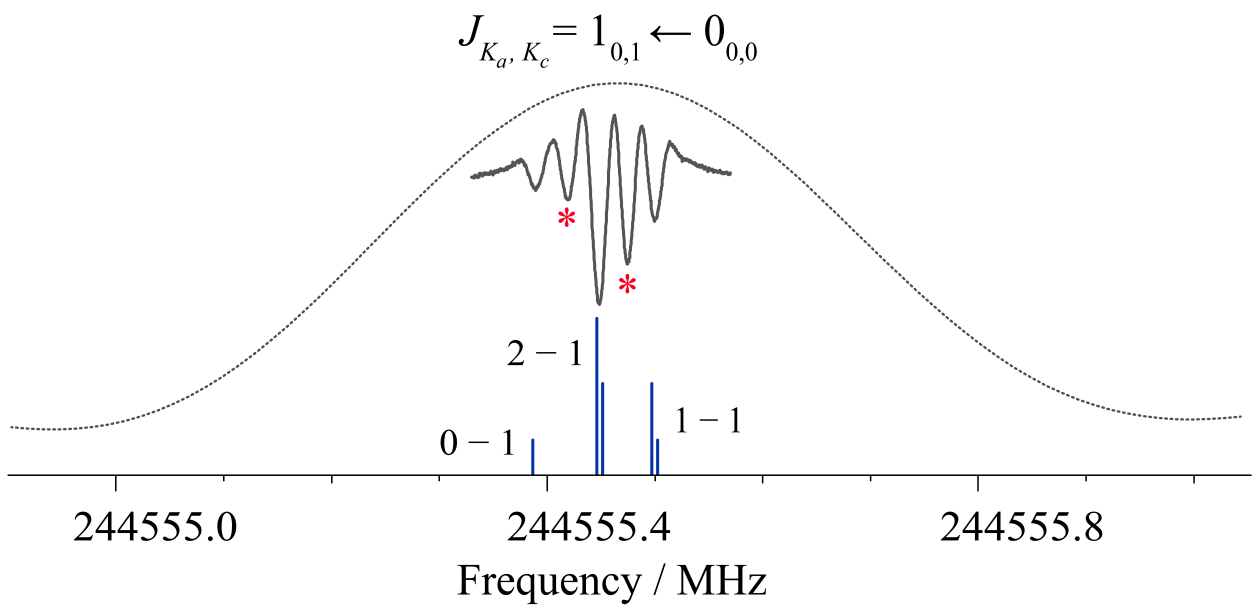

FIG. 1. Lamb-dip (solid black trace) and Doppler-limited (dashed black trace) spectra of the $J_{K_a,K_c} = 1_{0,1} \leftarrow 0_{0,0}$ transition of HDS observed around 244.555 GHz. The position and the relative intensity of the "real" transitions are represented as stick spectrum in blue, along with their $F_1 - F_1'$ quantum numbers. Red asterisks are used to mark "ghost" transitions. See text for details.

to the dipolar spin-spin coupling of deuterium and hydrogen. Overall, the hyperfine components of the rotational spectrum of HDS result from the selection rules $\Delta F_1, \Delta F = 0, \pm 1$, with F_1 and F being the quantum numbers originating from the coupling schemes $F_1 = J + I_D$ and $F = F_1 + I_H$. The reader is referred, for example, to refs. 19,100–102 for an account on these hyperfine interactions and, in particular, their impact on rotational spectra.

Figure 1 shows the $J_{K_a,K_c} = 1_{0,1} \leftarrow 0_{0,0}$ rotational transition[103] of HDS, which provides an example of a well-resolved hyperfine structure. The transition should appear as a triplet with the most-left, middle, and most-right dips corresponding to the $F_1 = 0-1$, $2-1$, and $1-1$ components, respectively. In this figure, the appearance of two crossover resonances, also denoted as "ghost transitions", is evident. These resonances are experimental artefacts due to the saturation of overlapping Gaussian profiles of two or more transitions with a common rotational energy level.[104,105] A detailed description of the procedure to account for them in the predicted rotational spectrum can be found in refs. 21,106.

The transition frequencies were retrieved from the recorded spectra by means of a line-profile analysis using the Lorentzian function and the Voigt profile model for Lamb-dip and Doppler-limited measurements, respectively.[107] In all cases, the frequency values were obtained as averages of several sets of measurements, with the experimental uncertainties (ranging from 1 to 300 kHz) derived on the basis of the standard deviations of the averages themselves, the line widths, and the signal-to-noise ratio of the spectra. As anticipated in Section II, the assignment of the observed hyperfine components to the correct transitions has been guided by spectra simulated on the basis of the computed values of the hyperfine parameters.

B. Watson-type Hamiltonian analysis

The newly recorded rotational transitions (271 distinct frequencies) have been merged with the ground-state MW and FIR data available in the literature[51–55] and analyzed in a combined fit where each transition was weighted proportionally to the inverse square of its experimental uncertainty. The least-squares fitting procedure has been performed with the `SPFIT` subroutine of the `CALPGM` suite of program.[108]

Tables I and II collect the results of the fit, which has been performed using a S-reduced Watson Hamiltonian[91] in the I^r representation.[100] In Table I, the experimental hyperfine parameters are compared with their computed counterparts, obtained as described in the Computational details section. As expected on the basis of the literature on this topic (see, e.g., refs. 13,19,21,22,109), agreement within the experimental error is noted, the only exception being the C_{aa}(H) constant for which a deviation of 4.7% is observed. In view of the high level of theory employed, the only possible source of discrepancy lies in non-negligible relativistic effects. Indeed, in ref. 110, it has been demonstrated that they can affect the computed spin-rotation constants of hydrogen by several percents (up to ~ 9 %). Overall, the results of Table I confirm the good accuracy that can be achieved with the Lamb-dip technique as well as the capability of high-level quantum-chemical calculations to provide quantitative predictions even for small hyperfine parameters.

Table II reports the experimental and computed rotational and centrifugal distortion constants, determined in this work, in comparison with previous experimental results.[55] For the rotational constants, a very good agreement between theory and experiment is observed (deviations of 0.03 %), thus confirming the high quality of the computed equilibrium structure which, as well-known, provides the largest contribution (about 99%) to the rotational constants.[19,111] Differently, the quartic and sextic centrifugal distortion terms show on average deviations, which are on the order of 7 % and 19 %, respectively. While these findings are surely connected to the small magnitude of these parameters, the discrepancies seem to indicate that vibrational corrections to these constants might be significant for floppy systems such as HDS and cannot be ignored. In this regard, it should be recalled that a perturbative formulation for the evaluation of vibrational contributions to the centrifugal-distortion terms has not been worked out and implemented yet. Thus, these computed quantities are equilibrium values, whereas our spectral analysis provides vibrational ground-state values.

A comparison with the previous analysis from ref. 55 reveals significant improvements in the accuracy of all spectroscopic constants. To give an example, the uncertainties of the rotational constants are reduced by three orders of magnitude and those on the centrifugal-distortion terms by one to two orders of magnitude. Moreover, five additional octic and decic constants have been determined for the first time. Consequently, the newly derived set of spectroscopic parameters will enable the accurate prediction of the rotational spectrum of HDS at any frequency up to the FIR region and the accurate modeling of the hyperfine structure produced by the deuterium and hydrogen nuclei.

TABLE II. Rotational and centrifugal-distortion constants of HDS.

Constant	Unit	Experiment[a]	Theory[b]	Previous[a,c]
A	MHz	292358.4209(4)	292279.55	292358.2(3)
B	MHz	147820.0874(2)	147790.71	147820.4(1)
C	MHz	96740.0613(1)	96772.95	96740.0(1)
D_J	MHz	1.171612(6)	1.212	1.1739(9)
D_{JK}	MHz	37.29440(2)	34.899	37.280(4)
D_K	MHz	-18.43210(4)	-18.002	-18.43(1)
d_1	MHz	-0.846074(3)	-0.761	-0.8485(3)
d_2	MHz	-0.721540(1)	-0.616	-0.7220(2)
H_J	kHz	-0.27102(7)	-0.232	-0.256(2)
H_{JK}	kHz	4.8548(4)	5.823	4.77(3)
H_{KJ}	kHz	12.099(2)	8.599	11.81(7)
H_K	kHz	-11.107(2)	-9.839	-10.9(1)
h_1	kHz	-0.05912(4)	-0.054	-0.0432(9)
h_2	kHz	0.17400(2)	0.133	0.180(1)
h_3	kHz	0.09653(1)	0.070	0.0978(5)
L_J	Hz	0.0317(2)		
L_{JJK}	Hz	0.241(1)		0.3(1)
L_{JK}	Hz	-8.98(1)		-7.1(4)
L_{KKJ}	Hz	4.50(4)		3.7(6)
L_K	Hz	-1.07(4)		-1.6(9)
l_1	mHz	31.4(1)		
l_2	mHz	-8.84(9)		-25.(3)
l_3	mHz	-40.32(7)		-45.(2)
l_4	mHz	-17.93(5)		-14.8(5)
P_{KJ}	mHz	11.3(1)		
P_{KKJ}	mHz	-16.7(3)		
P_K	mHz	9.8(3)		3.(2)
p_4	μHz	10.2(2)		
p_5	μHz	3.58(6)		3.(2)
Data		860		354
J_{max}, $K_{a\,max}$		22, 14		22, 14
MW–THz rms	kHz	60.2		
FIR rms	cm^{-1}	2.7E-4		2.6E-4
St. Dev.		1.08		1.08

[a] Numbers in parentheses are one standard deviation in units of the last quoted digit. **[b]** This work. **[c]** Ref. 55. Re-analyzed using the S reduction.

C. MARVEL analysis

MARVEL is an algorithm based on the concept of spectroscopic networks.[65,112–114] The MARVEL procedure allows the derivation of accurate ro-vibrational energy levels and associated uncertainties by inverting the information contained in a database of experimental transition frequencies. In the last decade, this protocol has been successfully applied to numerous molecular systems[115–121] and has been demonstrated to be, for small molecules, an alternative approach for predicting frequencies and associated uncertainties of molecular transitions.

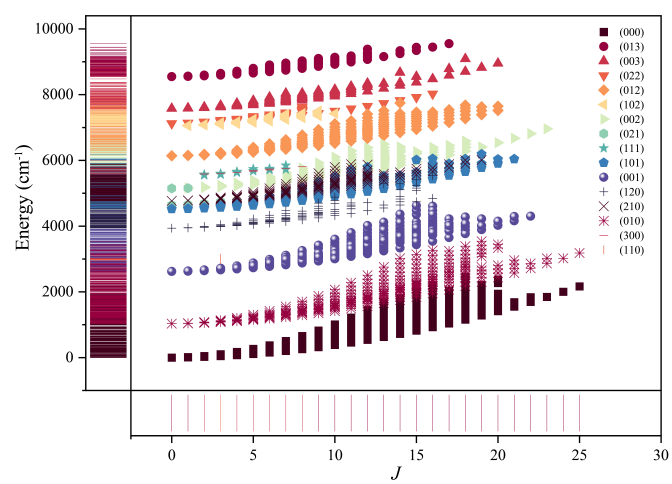

FIG. 2. Schematic representation of the MARVEL energy levels derived from our analysis. Each vibrational state is represented by a different symbol, for which a legend is provided using the format $(v_1 v_2 v_3)$.

TABLE III. Data sources used in the MARVEL analysis and their characteristics.

Tag	Ref.	Range (cm^{-1})	A/V[a]	MiU[b] (cm^{-1})	MaU[c] (cm^{-1})	AvU[d] (cm^{-1})
51HiSt	51	0.265 – 2.520	12 / 12	3.3E-7	3.3E-7	3.3E-7
70Burrus	53	5.110 – 11.117	6 / 6	3.3E-7	3.3E-7	3.3E-7
71HeCoDe	53	3.679 – 20.948	27 / 27	3.3E-7	3.3E-7	3.3E-7
73Stee	54	0.280 – 1.426	5 / 5	2.0E-6	3.0E-6	2.6E-6
23MeJiGaPu	This work	8.157 – 53.038	223 / 223	3.0E-8	1.0E-5	1.4E-6
85CaFlLeJo	55	25.184 – 267.612	535 / 535	2.0E-4	9.0E-4	2.3E-4
95UlToMeKo	56	2585.042 – 2980.261	69 / 69	1.0E-3	1.0E-3	1.0E-3
19SyUlBeGr	57	690.089 – 1511.468	2282 / 2282	1.0E-3	1.0E-3	1.0E-3
19UlBeGrRa	58	2006.402 – 2939.482	1532 / 1532	1.0E-3	1.0E-3	1.0E-3
06UlLiBeOn	59	3731.728 – 7219.680	2520 / 2520	2.0E-3	2.0E-3	2.0E-3
05LiGaChQi	60	4951.018 – 8662.091	3379 / 2891	2.0E-3	2.0E-3	2.0E-3

[a] Number of assigned/validated transitions. **[b]** Minimum uncertainty. **[c]** Maximum uncertainty. **[d]** Average uncertainty.

1. Quantum-number labeling

Each transition contained in a MARVEL input database must possess (i) an unambiguous labeling for the upper and lower states involved in the transition, (ii) the transition frequency together with its experimental uncertainty, and (iii) a unique tag which typically provides information about the literature source.

HDS is a triatomic asymmetric-top molecule isomorphic to the C_s point group. Therefore, six quantum numbers are required to uniquely label its ro-vibrational energy levels: the vibrational quantum numbers, in which v_1 represents the S−D stretching, v_2 the bending mode, and v_3 the S−H stretching, and the standard rotational quantum numbers, J, K_a, and K_c, for an asymmetric rotors. Since the hyperfine structure was not resolved in most of the literature data, we ignore its contribution in the present treatment and thus do not use the F_1 and F quantum numbers. For the same reason, hyperfine-resolved transitions are not included in our MARVEL data set but they are provided in a separate file in the Supplementary Material.

2. Experimental sources

All suitable ro-vibrational data of HDS have been collected from the literature. Besides the pure rotational transitions employed in our spectral analysis (§ IV B),[51–55] the majority of spectroscopic data concerns ro-vibrational bands observed across the whole mid-infrared and near-infrared regions.[56–64] Most of the spectroscopic data of HDS published before 2010 were collected in the W@DIS database (wadis.saga.iao.ru); they have been downloaded and converted in order to match the required format of the MARVEL input file. The remaining data have been taken directly from the original papers whenever the experimental line list was made available; for a few sources (namely refs. 61–64), we were not able to obtain the list of observed transitions and therefore they have not been incorporated in the analysis.

In total, our MARVEL database contains 10 sources of experimental transitions from the literature plus the newly measured transitions from this work. Table III presents a summary of all the data sources together with information concerning the investigated frequency range, the number of assigned and validated transitions (A/V), and the minimum/maximum/average experimental uncertainties (MiU/MaU/AvU).

3. Results

We have collected and analyzed 10590 experimental rotational and ro-vibrational transitions, 223 of which have been measured in this work. The list of all transitions is provided in the Supplementary Material. The main spectroscopic network contains 10057 validated transitions, which is about ~ 95 % of the entire data set. Nearly 500 transitions from ref. 60 (Tag: 05LiGaChQi) could not be validated in our analysis and are thus considered as misassigned; they appear with a negative wavenumber entry in our list in order to be ignored during the MARVEL analysis. To investigate the origin of such misassignments, we have also performed an effective Hamiltonian fit of the bands studied in 05LiGaChQi. We found that all discarded transitions are actually mislabeled and involve rotational levels with $K_a = 1$ and $K_a = 3$, either in the upper or lower level, most likely due to an eigenvalue re-ordering issue in the software used by 05LiGaChQi. Moreover, 45 transitions of our global database connect floating levels, which means that they are not linked to any level of the main spectroscopic network and, therefore, the energy of the corresponding levels could not be calculated.

A total number of 2541 active ro-vibrational energy levels have been derived together with statistically well-defined uncertainties. The highest ro-vibrational energy level is at 9552.886 cm^{-1} and belongs to the $v_2 + 3v_3$ combination state,

TABLE IV. Summary of the energy levels derived from the MARVEL analysis.[a]

State ($v_1 v_2 v_3$)	J range	K_a range	Levels	MiU – MaU (cm^{-1})	AvU (cm^{-1})	Energy Range (cm^{-1})
0 0 0	0 – 25	0 – 15	372	$<$ 0.0001 – 0.0071	0.0013	0.0000 – 2458.7271
0 0 1	0 – 22	0 – 14	293	0.0010 – 0.0064	0.0015	2621.4558 – 4624.0959
0 0 2	0 – 23	0 – 11	214	0.0020 – 0.0054	0.0023	5147.3553 – 6960.4715
0 0 3	0 – 20	0 – 7	130	0.0020 – 0.0050	0.0022	7577.8435 – 9089.2572
0 1 0	0 – 25	0 – 16	381	0.0010 – 0.0077	0.0019	1032.7151 – 3852.8277
0 1 2	0 – 20	0 – 12	219	0.0020 – 0.0050	0.0023	6139.7320 – 7744.0663
0 1 3	0 – 17	0 – 6	116	0.0020 – 0.0032	0.0021	8548.8927 – 9552.8861
0 2 1	0 – 19	0 – 8	97	0.0020 – 0.0048	0.0022	4638.8489 – 5893.7850
0 2 2	0 – 16	0 – 6	71	0.0020 – 0.0042	0.0021	7123.8864 – 8022.9404
1 0 1	0 – 21	0 – 11	227	0.0020 – 0.0057	0.0025	4522.6485 – 6187.8216
1 0 2	1 – 10	0 – 5	66	0.0020 – 0.0022	0.0020	7055.1149 – 7502.1927
1 1 0	3 – 3	0 – 3	7	0.0010 – 0.0010	0.0010	2971.5943 – 3027.4063
1 1 1	2 – 7	0 – 4	15	0.0020 – 0.0020	0.0020	5548.9136 – 5845.9678
1 2 0	0 – 16	0 – 10	131	0.0020 – 0.0046	0.0022	3938.6388 – 5541.4066
2 1 0	0 – 19	0 – 10	189	0.0020 – 0.0046	0.0022	4767.7069 – 6010.9407
3 0 0	2 – 8	0 – 1	12	0.0020 – 0.0020	0.0020	5583.5559 – 5809.1718

[a] Results are collected state-by-state. For the definition of the quantities, see notes of Table III.

while the highest rotational energy level of the vibrational ground state is the $J_{K_a,K_c} = 18_{14,4}$ level at 2458.727 cm^{-1}. The complete list of MARVEL energy levels is provided in the Supplementary Material, their average uncertainty being of the order of 2×10^{-3} cm^{-1}. A summary of the results of our MARVEL analysis is provided in Table IV, where the ranges of the J and K_a quantum numbers, energies, and uncertainties are provided for the 16 vibrational states investigated. A graphical representation of the derived energy levels is also given in Figure 2.

V. CONCLUSIONS

Light hydrides such as HDS represent important proxies for the investigation of interstellar environments, with molecular spectroscopy playing a major role for their identification. In this context, a thorough knowledge of the rotational spectrum across a widespread frequency domain and an accurate modeling of the hyperfine interactions that possibly affect the rotational spectrum are key prerequisites for deriving useful information from spectral line surveys of astronomical objects. In this work, we have addressed both issues by recording the millimeter- and submillimeter-wave spectra of HDS at an unprecedented resolution and combining the new measurements with the existing literature transitions into a global analysis. The fitting procedure of this large data set, ranging from centimeter-wave to well in the FIR region, allowed us to derive accurate rotational constants and to extend the centrifugal analysis to high-order terms. In addition, several hyperfine parameters have been determined with sub-kHz precision, thus enabling the simulation of the full hyperfine structure of the rotational spectrum when combined with theoretical predictions for those terms that are not experimentally determinable. For all hyperfine parameters, there is an excellent agreement between experiment and the theoretical counterpart, which has been computed at the highest possible level of theory. Overall, these results will permit to model the rotational spectrum of HDS from the MW to FIR region with remarkable accuracy, also by taking into account the effect of the subtle electric and magnetic interactions due to the deuterium and hydrogen nuclei. The latter effect has been demonstrated to be particularly important when retrieving molecular abundance from highly resolved astronomical observations, as this quantity can be overestimated by 5-20 % when the hyperfine structure is ignored.[26]

Furthermore, we have combined all the publicly available rotational and ro-vibrational transitions of HDS into a vast database and analyzed it by means of the MARVEL algorithm. Most of the experimental data ($\sim$ 95 %) have been successfully validated and led to the accurate determination of more than 2500 energy levels together with the associated uncertainties. All the empirical rotational-vibrational energy levels determined here constitute the first step toward the compilation of an extended line list of HDS, similarly to what is available for H_2S and its ^{33}S and ^{34}S isotopologues in the ExoMol[122] or HITRAN[123] databases. This line list will be useful for both atmospheric and astronomical studies.

ACKNOWLEDGMENTS

This work has been supported by MUR (PRIN Grant Number 202082CE3T) and by the University of Bologna (RFO

funds). NJ thanks the China Scholarships Council (CSC) for the financial support. The COST Action CA21101 "COSY - Confined molecular systems: from a new generation of materials to the stars" is also acknowledged. In Mainz, the work has been supported by the Deutsche Forschungsgemeinschaft (DFG) via grants GA 370/6-1 and 370/6-2.

DATA AVAILABILITY STATEMENT

The list of rotational and ro-vibrational transitions used in our analysis as well as the energy levels derived using the MARVEL algorithm are available as Supplementary Material.

[1] M. Ito, "Spectroscopy and dynamics of aromatic molecules having large-amplitude motions," J. Phys. Chem. **91**, 517–526 (1987).

[2] H. V. L. Nguyen and I. Kleiner, "Understanding (coupled) large amplitude motions: the interplay of microwave spectroscopy, spectral modeling, and quantum chemistry," Phys. Sci. Rev. (2020).

[3] F. Xie, N. A. Seifert, M. Heger, J. Thomas, W. Jäger, and Y. Xu, "The rich conformational landscape of perillyl alcohol revealed by broadband rotational spectroscopy and theoretical modelling," Phys. Chem. Chem. Phys. **21**, 15408–15416 (2019).

[4] W. G. Silva, T. Poonia, and J. van Wijngaarden, "Targeting the rich conformational landscape of N-allylmethylamine using rotational spectroscopy and quantum mechanical calculations," ChemPhysChem **21**, 2515–2522 (2020).

[5] M. Melosso, A. Melli, L. Spada, Y. Zheng, J. Chen, M. Li, T. Lu, G. Feng, Q. Gou, L. Dore, *et al.*, "Rich collection of n-propylamine and isopropylamine conformers: Rotational fingerprints and state-of-the-art quantum chemical investigation," J. Phys. Chem. A **124**, 1372–1381 (2020).

[6] W. G. Silva, G. Daudet, S. Perez, S. Thorwirth, and J. van Wijngaarden, "Conformational preferences of diallylamine: A rotational spectroscopic and theoretical study," J. Chem. Phys. **154**, 164303 (2021).

[7] F. Xie, N. A. Seifert, A. S. Hazrah, W. Jäger, and Y. Xu, "Conformational landscape, chirality recognition and chiral analyses: Rotational spectroscopy of tetrahydro-2-furoic acid $\cdots$ propylene oxide conformers," ChemPhysChem **22**, 455–460 (2021).

[8] C. Puzzarini, L. Spada, S. Alessandrini, and V. Barone, "The challenge of non-covalent interactions: theory meets experiment for reconciling accuracy and interpretation," J. Phys.: Condens. Matter **32**, 343002 (2020).

[9] W. Li, L. Spada, N. Tasinato, S. Rampino, L. Evangelisti, A. Gualandi, P. G. Cozzi, S. Melandri, V. Barone, and C. Puzzarini, "Theory meets experiment for noncovalent complexes: The puzzling case of pnicogen interactions," Angew. Chem. Int. Ed. **57**, 13853–13857 (2018).

[10] D. A. Obenchain, L. Spada, S. Alessandrini, S. Rampino, S. Herbers, N. Tasinato, M. Mendolicchio, P. Kraus, J. Gauss, C. Puzzarini, *et al.*, "Unveiling the sulfur–sulfur bridge: Accurate structural and energetic characterization of a homochalcogen intermolecular bond," Angew. Chem. Int. Ed. **57**, 15822–15826 (2018).

[11] H. Müller, P. Pracna, and V.-M. Horneman, "The $v_{10} = 1$ level of propyne, $H_3C{-}CCH$, and its interactions with $v_9 = 1$ and $v_{10} = 2$," J. Mol. Spectrosc. **216**, 397–407 (2002).

[12] L. Bizzocchi, F. Tamassia, J. Laas, B. M. Giuliano, C. Degli Esposti, L. Dore, M. Melosso, E. Canè, A. P. Charmet, H. S. Müller, *et al.*, "Rotational and high-resolution infrared spectrum of HC_3N: global ro-vibrational analysis and improved line catalog for astrophysical observations," Astrophys. J. Suppl. S. **233**, 11 (2017).

[13] M. Melosso, L. Dore, J. Gauss, and C. Puzzarini, "Deuterium hyperfine splittings in the rotational spectrum of NH_2D as revealed by lamb-dip spectroscopy," J. Mol. Spectrosc. **370**, 111291 (2020).

[14] M. Melosso, M. L. Diouf, L. Bizzocchi, M. E. Harding, F. M. Cozijn, C. Puzzarini, and W. Ubachs, "Hyperfine-resolved near-infrared spectra of H^{17}_2O," J. Phys. Chem. A **125**, 7884–7890 (2021).

[15] K. Yamada, "Resonance between ground and excited vibrational state due to centrifugal distortion coupling in the rotational spectrum of HNCO," J. Mol. Spectrosc. **81**, 139–151 (1980).

[16] L. H. Coudert, "Extreme anomalous centrifugal distortion in methylene," J. Chem. Phys. **153**, 144115 (2020).

[17] S. Urban and K. Yamada, "A breakdown of the Watson-type Hamiltonian for some asymmetric top molecules," J. Mol. Spectrosc. **160**, 279–288 (1993).

[18] I. Scivetti, J. Kohanoff, and N. I. Gidopoulos, "On the treatment of singularities of the Watson Hamiltonian for nonlinear molecules," Int. J. Quant. Chem. **111**, 307–317 (2011).

[19] C. Puzzarini, J. F. Stanton, and J. Gauss, "Quantum-chemical calculation of spectroscopic parameters for rotational spectroscopy," Int. Rev. Phys. Chem. **29**, 273–367 (2010).

[20] C. Puzzarini, J. Bloino, N. Tasinato, and V. Barone, "Accuracy and interpretability: The devil and the holy grail. new routes across old boundaries in computational spectroscopy," Chem. Rev. **119**, 8131–8191 (2019).

[21] C. Puzzarini, G. Cazzoli, M. E. Harding, J. Vázquez, and J. Gauss, "A new experimental absolute nuclear magnetic shielding scale for oxygen based on the rotational hyperfine structure of H^{17}_2O," J. Chem. Phys. **131**, 234304 (2009).

[22] T. Helgaker, J. Gauss, G. Cazzoli, and C. Puzzarini, "^{33}S hyperfine interactions in H_2S and SO_2 and revision of the sulfur nuclear magnetic shielding scale," J. Chem. Phys. **139**, 244308 (2013).

[23] G. Cazzoli, V. Lattanzi, J. L. Alonso, J. Gauss, and C. Puzzarini, "The hyperfine structure of the rotational spectrum of HDO and its extension to the THz region: accurate rest frequencies and spectroscopic parameters for astrophysical observations," Astrophys. J. **806**, 100 (2015).

[24] C. Puzzarini, G. Cazzoli, M. E. Harding, J. Vázquez, and J. Gauss, "The hyperfine structure in the rotational spectra of D^{17}_2O and $HD^{17}O$: Confirmation of the absolute nuclear magnetic shielding scale for oxygen," J. Chem. Phys. **142**, 124308 (2015).

[25] M. Melosso, L. Dore, F. Tamassia, C. L. Brogan, T. R. Hunter, and B. A. McGuire, "The submillimeter rotational spectrum of ethylene glycol up to 890 GHz and application to ALMA band 10 spectral line data of NGC 6334I," J. Phys. Chem. A **124**, 240–246 (2019).

[26] M. Melosso, L. Bizzocchi, L. Dore, Z. Kisiel, N. Jiang, S. Spezzano, P. Caselli, J. Gauss, and C. Puzzarini, "Improved centrifugal and hyperfine analysis of ND_2H and NH_2D and its application to the spectral line survey of L1544," J. Mol. Spectrosc. **377**, 111431 (2021).

[27] A. Cheung, D. M. Rank, C. Townes, D. D. Thornton, and W. Welch, "Detection of water in interstellar regions by its microwave radiation," Nature **221**, 626–628 (1969).

[28] B. Turner, B. Zuckerman, N. Fourikis, M. Morris, and P. Palmer, "Microwave detection of interstellar HDO," Astrophys. J. **198**, L125–L128 (1975).

[29] T. Jacq, P. Jewell, C. Henkel, C. Walmsley, and A. Baudry, "H_2(0-18) in hot dense molecular cloud cores," Astron. Astrophys. **199**, L5–L8 (1988).

[30] Å. Hjalmarson, P. Bergman, N. Biver, H.-G. Florén, U. Frisk, T. Hasegawa, K. Justtanont, B. Larsson, S. Lundin, M. Olberg, *et al.*, "Recent astronomy highlights from the Odin satellite," Adv. Space Res. **36**, 1031–1047 (2005).

[31] H. Butner, S. Charnley, C. Ceccarelli, S. Rodgers, J. Pardo, B. Parise, J. Cernicharo, and G. Davis, "Discovery of interstellar heavy water," Astrophys. J. **659**, L137 (2007).

[32] E. F. van Dishoeck, D. J. Jansen, P. Schilke, and T. Phillips, "Detection of the interstellar NH_2 radical," Astrophys. J. **416**, L83 (1993).

[33] M. Melosso, L. Bizzocchi, O. Sipilä, B. Giuliano, L. Dore, F. Tamassia, M.-A. Martin-Drumel, O. Pirali, E. Redaelli, and P. Caselli, "First detection of NHD and ND_2 in the interstellar medium. amidogen deuteration in iras 16293–2422," Astron. Astrophys. **641**, A153 (2020).

[34] J. M. Hollis, P. R. Jewell, and F. J. Lovas, "Confirmation of interstellar methylene," Astrophys. J. **438**, 259–264 (1995).

[35] P. Thaddeus, M. Kutner, A. Penzias, R. Wilson, and K. Jefferts, "Interstellar hydrogen sulfide," Astrophys. J. **176**, L73 (1972).

[36] Y. Minh, L. M. Ziurys, W. M. Irvine, and D. McGonagle, "Observations of the H_2S toward OMC-1," Astrophys. J. **360**, 136–141 (1990).

[37] C. Vastel, T. Phillips, C. Ceccarelli, and J. Pearson, "First detection of doubly deuterated hydrogen sulfide," Astrophys. J. **593**, L97 (2003).

[38] G. Macdonald, A. Gibb, R. Habing, and T. Millar, "A 330-360 GHz spectral survey of G34.3+0.15. I. Data and physical analysis," Astron. Astrophys. Suppl. S. **119**, 333–367 (1996).

[39] M. N. Drozdovskaya, E. F. van Dishoeck, J. K. Jørgensen, U. Calmonte, M. H. van der Wiel, A. Coutens, H. Calcutt, H. S. Müller, P. Bjerkeli, M. V.

Persson, *et al.*, "The ALMA-PILS survey: the sulphur connection between protostars and comets: IRAS 16293–2422 B and 67P/Churyumov–Gerasimenko," Mon. Not. R. Astron. Soc. **476**, 4949–4964 (2018).

[40]Y. Aikawa, V. Wakelam, F. Hersant, R. T. Garrod, and E. Herbst, "From prestellar to protostellar cores. II. Time dependence and deuterium fractionation," Astrophys. J. **760**, 40 (2012).

[41]H.-R. Chen, S.-Y. Liu, Y.-N. Su, and M.-Y. Wang, "Deuterium fractionation as an evolutionary probe in massive protostellar/cluster cores," Astrophys. J. **743**, 196 (2011).

[42]M. Emprechtinger, P. Caselli, N. Volgenau, J. Stutzki, and M. Wiedner, "The N_2D^+/N_2H^+ ratio as an evolutionary tracer of Class 0 protostars," Astron. Astrophys. **493**, 89–105 (2009).

[43]F. Fontani, A. Palau, P. Caselli, Á. Sánchez-Monge, M. Butler, J. Tan, I. Jiménez-Serra, G. Busquet, S. Leurini, and M. Audard, "Deuteration as an evolutionary tracer in massive-star formation," Astron. Astrophys. **529**, L7 (2011).

[44]E. Bianchi, C. Ceccarelli, C. Codella, J. Enrique-Romero, C. Favre, and B. Lefloch, "Astrochemistry as a tool to follow protostellar evolution: The class I stage," ACS Earth Space Chem. **3**, 2659–2674 (2019).

[45]R. Martín-Doménech, I. Jiménez-Serra, G. M. Caro, H. Müller, A. Occhiogrosso, L. Testi, P. Woods, and S. Viti, "The sulfur depletion problem: upper limits on the H_2S_2, HS_2, and S_2 gas-phase abundances toward the low-mass warm core IRAS 16293-2422," Astron. Astrophys. **585**, A112 (2016).

[46]C. Z. Palmer, R. C. Fortenberry, and J. S. Francisco, "Spectral signatures of hydrogen thioperoxide (HOSH) and hydrogen persulfide (HSSH): Possible molecular sulfur sinks in the dense ISM," Molecules **27**, 3200 (2022).

[47]D. E. Anderson, E. A. Bergin, S. Maret, and V. Wakelam, "New constraints on the sulfur reservoir in the dense interstellar medium provided by spitzer observations of S_i in shocked gas," Astrophys. J. **779**, 141 (2013).

[48]A. G. G. M. Tielens, "The molecular universe," Rev. Mod. Phys. **85**, 1021–1081 (2013).

[49]S. Yamamoto, *Introduction to Astrochemistry (Chemical Evolution from Interstellar Clouds to Star and Planet Formation)* (Springer, 2017).

[50]E. Herbst, "Unusual chemical processes in interstellar chemistry: Past and present," Front. Astron. Space Sci. **8**, 776942 (2021).

[51]R. Hillger and M. Strandberg, "Centrifugal distortion in asymmetric molecules. II. HDS," Phys. Rev. **83**, 575 (1951).

[52]P. Thaddeus, L. Krisher, and J. Loubser, "Hyperfine structure in the microwave spectrum of HDO, HDS, CH_2O, and CHDO: Beam-maser spectroscopy on asymmetric-top molecules," J. Chem. Phys. **40**, 257–273 (1964).

[53]P. Helminger, R. L. Cook, and F. C. De Lucia, "Microwave spectrum and centrifugal distortion effects of HDS," J. Mol. Spectrosc. **40**, 125–136 (1971).

[54]F. J. Lovas, "Microwave spectral tables II. Triatomic molecules," J. Phys. Chem. Ref. Data **7**, 1445–1750 (1978).

[55]C. Camy-Peyret, J.-M. Flaud, L. Lechuga-Fossat, and J. Johns, "The far-infrared spectrum of deuterated hydrogen sulfide: The ground state rotational constants of D^{32}_2S, D^{34}_2S, $HD^{32}S$, and $HD^{34}S$," J. Mol. Spectrosc. **109**, 300–333 (1985).

[56]O. N. Ulenikov, R. Tolchenov, E. Melekhina, M. Koivusaari, S. Alanko, and R. Anttila, "High resolution study of deuterated hydrogen sulfide in the region 2400–3000 cm^{-1}," J. Mol. Spectrosc. **170**, 397–416 (1995).

[57]C. Sydow, O. Ulenikov, E. Bekhtereva, O. Gromova, Z. Xintong, P. Glushkov, C. Maul, and S. Bauerecker, "Extended analysis of FTIR high resolution spectra of $HD^{32}S$ and $HD^{34}S$ in the region of the $\nu 2$ band: Positions and strengths of individual lines," J. Quant. Spectrosc. Ra. **225**, 286–300 (2019).

[58]O. Ulenikov, E. Bekhtereva, O. Gromova, N. Raspopova, C. Sydow, and S. Bauerecker, "Extended analysis of the $\nu 3$ band of $HD^{32}S$: Line positions, energies, and line strengths," J. Quant. Spectrosc. Ra. **230**, 131–141 (2019).

[59]O. N. Ulenikov, A.-W. Liu, E. S. Bekhtereva, G. Onopenko, O. V. Gromova, L. Wan, S.-M. Hu, and J.-M. Flaud, "Joint ro-vibrational analysis of the HDS high resolution infrared data," J. Mol. Spectrosc. **240**, 32–44 (2006).

[60]A.-W. Liu, B. Gao, G.-S. Cheng, F. Qi, and S.-M. Hu, "High-resolution rotational analysis of HDS: $2\nu 3$, $\nu 2+ 2\nu 3$, $3\nu 3$, and $\nu 2+ 3\nu 3$ bands," J. Mol. Spectrosc. **232**, 279–290 (2005).

[61]O. Ulenikov, R. Tolchenov, M. Koivusaari, S. Alanko, and R. Antilla, "Study of the fine rotational structure of the ν_2 band of HDS," J. Mol. Spectrosc. **170**, 1–9 (1995).

[62]V. G. Tyuterev, L. Régalia-Jarlot, D. W. Schwenke, S. A. Tashkun, and Y. G. Borkov, "Global variational calculations of high-resolution rovibrational spectra: isotopic effects, intensity anomalies and experimental confirmations for H_2S, HDS, D_2S molecules," C. R. Phys. **5**, 189–199 (2004).

[63]O. Ulenikov, G. Onopenko, I. Olekhnovitch, S. Alanko, V.-M. Horneman, M. Koivusaari, and R. Anttila, "High-resolution fourier transform spectra of hds in the regions of the bands ν_1 and $2\nu_1/\nu_2+ \nu_3$," J. Mol. Spectrosc. **189**, 74–82 (1998).

[64]O. Ulenikov, E. Ditenberg, I. Olekhnovitch, S. Alanko, M. Koivusaari, and R. Anttila, "Isotope substitution in near local mode molecules: Bending overtones $n\nu_2$ (n= 2, 3) of the HDS molecule," J. Mol. Spectrosc. **191**, 239–247 (1998).

[65]T. Furtenbacher, A. G. Császár, and J. Tennyson, "MARVEL: measured active rotational–vibrational energy levels," J. Mol. Spectrosc. **245**, 115–125 (2007).

[66]P. Pyykkö, "Year-2008 nuclear quadrupole moments," Mol. Phys. **106**, 1965–1974 (2008).

[67]J. Gauss, K. Ruud, and T. Helgaker, "Perturbation-dependent atomic orbitals for the calculation of spin-rotation constants and rotational g tensors," J. Chem. Phys. **105**, 2804 (1996).

[68]J. Gauss and D. Sundholm, "Coupled-cluster calculations of spin-rotation constants," Mol. Phys. **91**, 449–458 (1997).

[69]C. Puzzarini, "Ab initio characterization of XH_3 (X = N,P). Part II. Electric, magnetic and spectroscopic properties of ammonia and phosphine," Theor. Chem. Acc. **121**, 1–10 (2008).

[70]I. Shavitt and R. J. Bartlett, *Many-body methods in chemistry and physics: MBPT and coupled-cluster theory* (Cambridge University Press, 2009).

[71]K. Raghavachari, G. W. Trucks, J. A. Pople, and M. Head-Gordon, "A fifth-order perturbation comparison of electron correlation theories," Chem. Phys. Lett. **157**, 479–483 (1989).

[72]T. H. Dunning Jr., "Gaussian Basis Sets for Use in Correlated Molecular Calculations. I. The Atoms Boron through Neon and Hydrogen," J. Chem. Phys. **90**, 1007 (1989).

[73]A. Kendall, T. H. Dunning Jr., and R. J. Harrison, "Electron affinities of the first-row atoms revisited. Systematic basis sets and wave functions ," J. Chem. Phys. **96**, 6796 (1992).

[74]D. E. Woon and T. H. Dunning Jr., "Gaussian basis sets for use in correlated molecular calculations. V. Core-valence basis sets for boron through neon," J. Chem. Phys. **103**, 4572 (1995).

[75]K. A. Peterson and T. H. Dunning Jr., "Accurate correlation consistent basis sets for molecular core-valence correlation effects: The second row atoms al-ar, and the first row atoms b-ne revisited," J. Chem. Phys. **117**, 10548–10560 (2002).

[76]I. M. Mills, "Molecular Spectroscopy: Modern Research, ed. KN Rao and CW Matthews," (1972).

[77]A. A. Auer, J. Gauss, and J. F. Stanton, "Quantitative prediction of gas-phase ^{13}C nuclear magnetic shielding constants," J. Chem. Phys. **118**, 10407–10417 (2003).

[78]D. Feller, "The use of systematic sequences of wave functions for estimating the complete basis set, Full Configuration Interaction limit in water," J. Chem. Phys. **98**, 7059 (1993).

[79]T. Helgaker, W. Klopper, H. Koch, and J. Noga, "Basis-set convergence of correlated calculations on water," J. Chem. Phys. **106**, 9639 (1997).

[80]J. Noga and R. J. Bartlett, "The full CCSDT model for molecular electronic structure," J. Chem. Phys. **86**, 7041–7050 (1987).

[81]G. E. Scuseria and H. F. Schaefer, "A new implementation of the full CCSDT model for molecular electronic structure," Chem. Phys. Lett. **152**, 382–386 (1988).

[82]S. A. Kucharski and R. J. Bartlett, "The coupled-cluster single, double, triple, and quadruple excitation method," J. Chem. Phys. **97**, 4282–4288 (1992).

[83]M. Kállay and P. Surján, "Higher excitations in coupled-cluster theory," J. Chem. Phys. **115**, 2945–2954 (2001).

[84]A. K. Wilson, T. van Mourik, and T. H. Dunning Jr, "Gaussian basis sets for use in correlated molecular calculations. VI. Sextuple zeta correlation consistent basis sets for boron through neon," J. Mol. Struct. THEOCHEM **388**, 339–349 (1996).

[85]T. Van Mourik, A. K. Wilson, and T. H. Dunning Jr, "Benchmark calculations with correlated molecular wavefunctions. XIII. Potential energy curves for He_2, Ne_2 and Ar_2 using correlation consistent basis sets through augmented sextuple zeta," Mol. Phys. **96**, 529–547 (1999).

[86]W. Kutzelnigg, *Relativistic Electronic Structure Theory. Part I. Fundamentals*, edited by P. Schwerdtfeger (Elsevier, Amsterdam, 2002).

[87]G. Cazzoli, C. Puzzarini, and J. Gauss, "Rare isotopic species of hydrogen sulfide: the rotational spectrum of H^{36}_2S," Astron. Astrophys. **566**, A52 (2014).

[88]J. Gauss and J. Stanton, Chem. Phys. Lett. **276**, 70–76 (1997).

[89]W. Schneider and W. Thiel, Chem. Phys. Lett. **157**, 367–373 (1989).

[90]J. F. Stanton, C. L. Lopreore, and J. Gauss, J. Chem. Phys. **108**, 7190–7196 (1998).

[91]J. K. G. Watson, "Aspects of quartic and sextic centrifugal effects on rotational energy levels," in *Vibrational Spectra and Structure*, Vol. 6, edited by J. Durig (Elsevier, Amsterdam, 1977) pp. 1–89.

[92]J. F. Stanton, J. Gauss, L. Cheng, M. E. Harding, D. A. Matthews, and P. G. Szalay, "CFOUR, coupled-cluster techniques for computational chemistry, a quantum-chemical program package," With contributions from A. Asthana, A.A. Auer, R.J. Bartlett, U. Benedikt, C. Berger, D.E. Bernholdt, S. Blaschke, Y. J. Bomble, S. Burger, O. Christiansen, D. Datta, F. Engel, R. Faber, J. Greiner, M. Heckert, O. Heun, M. Hilgenberg, C. Huber, T.-C. Jagau, D. Jonsson, J. Jusélius, T. Kirsch, M.-P. Kitsaras, K. Klein, G.M. Kopper, W.J. Lauderdale, F. Lipparini, J. Liu, T. Metzroth, L.A. Mück, D.P. O'Neill, T. Nottoli, J. Oswald, D.R. Price, E. Prochnow, C. Puzzarini, K. Ruud, F. Schiffmann, W. Schwalbach, C. Simmons, S. Stopkowicz, A. Tajti, J. Vázquez, F. Wang, J.D. Watts, C. Zhang, X. Zheng, and the integral packages MOLECULE (J. Almlöf and P.R. Taylor), PROPS (P.R. Taylor), ABACUS (T. Helgaker, H.J. Aa. Jensen, P. Jørgensen, and J. Olsen), and ECP routines by A. V. Mitin and C. van Wüllen. For the current version, see http://www.cfour.de.

[93]D. A. Matthews, L. Cheng, M. E. Harding, F. Lipparini, S. Stopkowicz, T.-C. Jagau, P. G. Szalay, J. Gauss, and J. F. Stanton, "Coupled-cluster techniques for computational chemistry: The CFOUR program package," J. Chem. Phys. **152**, 214108 (2020).

[94]M. Kállay, "MRCC, a generalized CC/CI program," For the current version, see http://www.mrcc.hu.

[95]M. Kállay, P. R. Nagy, D. Mester, Z. Rolik, G. Samu, J. Csontos, J. Csóka, P. B. Szabó, L. Gyevi-Nagy, B. Hégely, I. Ladjánszki, L. Szegedy, B. Ladóczki, K. Petrov, M. Farkas, P. D. Mezei, and A. Ganyecz, "The MRCC program system: Accurate quantum chemistry from water to proteins," J. Chem. Phys. **152**, 074107 (2020).

[96]C. Puzzarini, G. Cazzoli, and J. Gauss, "The rotational spectra of $HD^{17}O$ and D^{17}_2O: Experiment and quantum-chemical calculations," J. Chem. Phys. **137**, 154311 (2012).

[97]M. Melosso, C. Degli Esposti, and L. Dore, "Terahertz spectroscopy and global analysis of the rotational spectrum of doubly deuterated amidogen radical ND_2," Astrophys. J. Suppl. S. **233**, 15 (2017).

[98]M. Melosso, L. Bizzocchi, F. Tamassia, C. Degli Esposti, E. Canè, and L. Dore, "The rotational spectrum of ^{15}ND. Isotopic-independent Dunham-type analysis of the imidogen radical," Phys. Chem. Chem. Phys. **21**, 3564–3573 (2019).

[99]G. Cazzoli and C. Puzzarini, "Sub-Doppler Resolution in the THz Frequency Domain: 1 kHz Accuracy at 1 THz by Exploiting the Lamb-Dip Technique," J. Phys. Chem. A **117**, 13759–13766 (2013).

[100]W. Gordy and R. L. Cook, *Microwave Molecular Spectra* (Wiley, 1984).

[101]W. H. Flygare, "Magnetic interactions in molecules and an analysis of molecular electronic charge distribution from magnetic parameters," Chem. Rev. **74**, 653–687 (1974).

[102]C. Puzzarini, "Rotational spectroscopy meets theory," Phys. Chem. Chem. Phys. **15**, 6595–6607 (2013).

[103]J is the quantum number for the total angular momentum, while K_a and K_c are pseudo-quantum numbers associated to the projections of the angular moment along the a-axis and c-axis in the prolate- and oblate-top limits, respectively.

[104]R. S. Winton, *Observations and Applications of the Lamb-dip in Millimeter-Wave Molecular Spectroscopy, Ph.D. dissertation* (Duke University, Durham, 1972).

[105]V. S. Letokhov and V. P. Chebotayev, *Nonlinear Laser Spectroscopy* (Springer-Verlag, Berlin/Heidelberg/New York, 1977).

[106]G. Cazzoli and C. Puzzarini, "The Lamb-dip spectrum of the $J+1 \leftarrow J$ ($J = 0, 1, 3-8$) transitions of $H^{13}CN$: The nuclear hyperfine structure due to H, ^{13}C, and ^{14}N," J. Mol. Spectrosc. **233**, 280–289 (2005).

[107]L. Dore, "Using Fast Fourier Transform to compute the line shape of frequency-modulated spectral profiles," J. Mol. Spectrosc. **221**, 93–98 (2003).

[108]H. M. Pickett, "The fitting and prediction of vibration-rotation spectra with spin interactions," J. Mol. Spectrosc. **148**, 371–377 (1991).

[109]G. Cazzoli, C. Puzzarini, M. E. Harding, and J. Gauss, "The hyperfine structure in the rotational spectrum of water: Lamb-dip technique and quantum-chemical calculations," Chemical Physics Letters **473**, 21–25 (2009).

[110]S. Komorovsky, M. Repisky, E. Malkin, K. Ruud, and J. Gauss, "Communication: The absolute shielding scales of oxygen and sulfur revisited," J. Chem. Phys. **142**, 091102 (2015).

[111]C. Puzzarini, J. F. Stanton, and J. Gauss, "Quantum-chemical calculation of spectroscopic parameters for rotational spectroscopy," Int. Rev. Phys. Chem. **29**, 273–367 (2010).

[112]T. Furtenbacher and A. G. Császár, "On employing H^{16}_2O, H^{17}_2O, H^{18}_2O, and D^{16}_2O lines as frequency standards in the 15–170 cm^{-1} window," J. Quant. Spectrosc. Ra. **109**, 1234–1251 (2008).

[113]T. Furtenbacher and A. G. Császár, "The role of intensities in determining characteristics of spectroscopic networks," J. Mol. Struct. **1009**, 123–129 (2012).

[114]T. Furtenbacher and A. G. Csaszar, "MARVEL: measured active rotational–vibrational energy levels. II. Algorithmic improvements," J. Quant. Spectrosc. Ra. **113**, 929–935 (2012).

[115]T. Furtenbacher, T. Szidarovszky, E. Mátyus, C. Fábri, and A. G. Császár, "Analysis of the rotational–vibrational states of the molecular ion H_3^+," J. Chem. Theory Comput. **9**, 5471–5478 (2013).

[116]T. Furtenbacher, T. Szidarovszky, C. Fábri, and A. G. Császár, "MARVEL analysis of the rotational–vibrational states of the molecular ions H_2D^+ and D_2H^+," Phys. Chem. Chem. Phys. **15**, 10181–10193 (2013).

[117]A. R. Al Derzi, T. Furtenbacher, J. Tennyson, S. N. Yurchenko, and A. G. Császár, "MARVEL analysis of the measured high-resolution spectra of $^{14}NH_3$," J. Quant. Spectrosc. Ra. **161**, 117–130 (2015).

[118]L. K. McKemmish, T. Masseron, S. Sheppard, E. Sandeman, Z. Schofield, T. Furtenbacher, A. G. Császár, J. Tennyson, and C. Sousa-Silva, "MARVEL analysis of the measured high-resolution rovibronic spectra of $^{48}Ti^{16}O$," Astrophys. J. Suppl. S. **228**, 15 (2017).

[119]R. Tóbiás, T. Furtenbacher, A. G. Császár, O. V. Naumenko, J. Tennyson, J.-M. Flaud, P. Kumar, and B. Poirier, "Critical evaluation of measured rotational–vibrational transitions of four sulphur isotopologues of $S^{16}O_2$," J. Quant. Spectrosc. Ra. **208**, 152–163 (2018).

[120]A. R. Al-Derzi, J. Tennyson, S. N. Yurchenko, M. Melosso, N. Jiang, C. Puzzarini, L. Dore, T. Furtenbacher, R. Tóbiás, and A. G. Császár, "An improved rovibrational linelist of formaldehyde, $H^{12}_2C^{16}O$," J. Quant. Spectrosc. Ra. **266**, 107563 (2021).

[121]T. M. Mellor, A. Owens, J. Tennyson, and S. N. Yurchenko, "MARVEL analysis of high-resolution spectra of thioformaldehyde (H_2CS)," J. Mol. Spectrosc. **391**, 111732 (2023).

[122]A. A. Azzam, J. Tennyson, S. N. Yurchenko, and O. V. Naumenko, "ExoMol molecular line lists–XVI. The rotation–vibration spectrum of hot H_2S," Mon. Not. R. Astron. Soc. **460**, 4063–4074 (2016).

[123]I. Gordon, L. Rothman, R. Hargreaves, R. Hashemi, E. Karlovets, F. Skinner, E. Conway, C. Hill, R. Kochanov, Y. Tan, *et al.*, "The HITRAN2020 molecular spectroscopic database," J. Quant. Spectrosc. Ra. **277**, 107949 (2022).